



PII: S0364-5916(02)00025-1

### **A Thermodynamic Assessment of the Cu-Mg-Ni Ternary System**

S. GORSSE\* and G. J. SHIFLET\*\*

Department of Materials Science and Engineering  
University of Virginia  
Charlottesville, VA 22902

\*Systran Federal Corp., Dayton, OH 45431

\*\*Corresponding author's e-mail: gjs@virginia.edu

(Received October 27, 2001)

**Abstract:** A complete thermodynamic description of the Cu-Mg-Ni ternary system was carried out based on the CALPHAD method. Ternary solubilities of the binary phases  $Mg_2Cu$ ,  $Cu_2Mg$ ,  $Mg_2Ni$  and  $Ni_2Mg$  were considered. The Gibbs energies of these semi-stoichiometric compounds were expressed by the compound-energy formalism. Liquid and solid solution phases were described using the Redlich-Kister-Muggiani formalism. The model parameters were evaluated using ThermoCalc software, utilizing the experimental data available in the literature including experimental thermodynamic functions and previously established portions of the phase diagram, such as isopleths and isotherms. Reasonable agreement was obtained between calculated results and experimental information. © 2002 Published by Elsevier Science Ltd.

#### **1. Introduction:**

The present work is part of an effort to understand and possibly extend the Al-Cu-Mg-Ni system to produce bulk amorphous aluminum alloys and understand subsequent devitrification. Amorphous alloys offer the real potential for a dramatic improvement of the metallic alloy specific strength. Further, strength and ductility may be increased by controlled partial recrystallization of the fully amorphous Al alloys.

The Al-Cu-Mg-Ni alloy system is of interest because some compositions can be quenched, by melt spinning, into a fully amorphous phase presenting encouraging ductility [1]. The Ni element exerts a very pronounced influence upon the glass formability, due to the unique atomic configuration between Al and Ni atoms [1].

The goal of this work is to provide a complete thermodynamic description of the Al-Cu-Mg-Ni system, enabling a better understanding of the Ni effect and as a tool to predict phase transformations to control the alloy microstructure during the recrystallization. In order to obtain a thermodynamic description of the quaternary system, it is necessary to first develop descriptions for the four ternary sub-systems.

The present paper is therefore concerned with the thermodynamic assessment of the ternary Cu-Mg-Ni system. This assessment has been performed while insuring compatibility in phase modeling with the existing thermodynamic description of the Al-Cu-Mg system developed by Buhler et al. [2], which is believed to be reliable. Because of the lack of experimental data and the fact that we are mainly interested in Al-rich alloys, the purpose of the present work is primarily to propose a description offering consistency between the thermodynamic data and the suggested phase diagram.

## 2. Review of experimental data available for the Cu-Mg-Ni system:

### 2.1. Binary subsystems:

The descriptions of the binary systems were taken from the literature. In Figs. 1-3 the three binary systems are presented; there are four intermetallic compounds in addition of the solution phases (Liquid, FCC-A1 and HCP-A3).

The thermodynamic description of the Cu-Mg system was carried out by Coughanowr et al. [3], then Buhler et al. [2, 4]. In their description,  $\text{Cu}_2\text{Mg}$  was chosen to be a Wagner-Schottky type phase, taking into consideration the range of homogeneity, and  $\text{Mg}_2\text{Cu}$  as a stoichiometric compound (Fig. 1).

Complete assessment of the Mg-Ni system was performed by Jacobs and Spencer [5]. The Mg-Ni system consists of the liquid,  $\text{Mg}_2\text{Ni}$ ,  $\text{Ni}_2\text{Mg}$ , and the terminal solid solutions HCP-A3 and FCC-A1 (Fig. 2).  $\text{Mg}_2\text{Ni}$  was treated as a stoichiometric compound,  $\text{Ni}_2\text{Mg}$  with a narrow homogeneity range, and the solubility of Mg in the FCC phase and Ni in the HCP phase were neglected.

The Cu-Ni phase diagram is an isomorphous one, with complete range of liquid and solid solution (Fig. 3). At low temperatures (just below 600 K), a miscibility gap is present. For the present work the assessment of Jansson [6] was used.

### 2.2. Ternary system:

No ternary compounds were identified but important ternary solubilities of the binary compounds have been reported in the literature. In this section, the critical experimental information is presented.

#### *Phase diagram data:*

The compounds present in the Cu-Mg and Mg-Ni sub-systems are extended to the ternary system. Investigations of Koster [7] and Mikheeva and Babayan [8] suggested a complete series of solid solutions exist in the  $\text{Cu}_2\text{Mg}$ - $\text{Ni}_2\text{Mg}$  quasibinary and a continuous monovariant eutectic trough extends between the Ni- $\text{Ni}_2\text{Mg}$  and Cu- $\text{Cu}_2\text{Mg}$  eutectics.

But work of Lieser and Witte [9], based on microscopic and electron microprobe analysis, indicates the existence of a peritectic reaction between  $\text{Cu}_2\text{Mg}$  and  $\text{Ni}_2\text{Mg}$ . The same authors determined the solidus and liquidus boundaries of the quasibinary  $\text{Cu}_2\text{Mg}$ - $\text{Ni}_2\text{Mg}$  system and suggested that the solubility of Ni in  $\text{Cu}_2\text{Mg}$  is about 26 at.% and Cu in  $\text{Ni}_2\text{Mg}$  about 25 at.%.

Fehrenbach et al. [10] reported that alloys homogenized at 1073 K and containing respectively 35 at.% Ni, 48 Cu, 17 Mg, and 46 at.%Ni, 39 Cu, 15 Mg, consisted of three phases FCC-A1,  $\text{Ni}_2\text{Mg}$  and  $\text{Cu}_2\text{Mg}$ . Microprobe electron analysis indicated a solubility of Cu in  $\text{Ni}_2\text{Mg}$  of 3-5 at.%, much lower than claimed by Lieser [9]. Also Fehrenbach et al. located the monovariant eutectic trough extending between the binary eutectic Cu- $\text{Cu}_2\text{Mg}$  and Ni- $\text{Ni}_2\text{Mg}$  into the ternary alloy system for alloys containing up to 25 at.% Ni, and determined liquidus and solidus boundaries along this eutectic trough using thermal analysis [10]. In the same work the presence of a peritectic reaction in the  $\text{Cu}_2\text{Mg}$ - $\text{Ni}_2\text{Mg}$  quasibinary system was confirmed by microscopy and microprobe analysis, the solubility of Ni in  $\text{Cu}_2\text{Mg}$  was reported at 20 at.%. In accordance with these experimental results, they proposed four isothermal sections at 1003, 1073, 1081 and 1123 K.

Ipsier et al. [11] also confirmed the presence of a peritectic reaction between  $\text{Cu}_2\text{Mg}$  and  $\text{Ni}_2\text{Mg}$  and estimated the solubility of Cu in  $\text{Ni}_2\text{Mg}$  to be 5% between 931 and 1203 K, as suggested previously by Fehrenbach et al. [10]. Furthermore their results indicate that the Ni content in  $\text{Cu}_2\text{Mg}$  must be higher than 22 at.%.

Karonik et al. [12] studied the phase equilibria at 673 K in the Mg-rich corner. Three phase equilibrium was established that involves HCP,  $\text{Mg}_2\text{Ni}$  and  $\text{Mg}_2\text{Cu}$ . The maximum solubility of Cu in  $\text{Mg}_2\text{Ni}$  was found at

25 at.%, and the Ni in Mg<sub>2</sub>Cu did not exceed 3 at.%. The width of the ternary extension of Mg<sub>2</sub>Ni was estimated to be not larger than 0.5 at.%. The solubility of Cu and Ni in HCP appeared to be negligible.

Results from Ipsier et al. [11] are in very good agreement with those by Karonik [12]. Measurements performed in the section with a content of 71 at.% Mg, indicated that the boundary between two-phase (HCP + Mg<sub>2</sub>Ni) and three phase fields (HCP + Mg<sub>2</sub>Ni + Mg<sub>2</sub>Cu) is at 22 at.% Cu for 723 K. Extrapolating to 66.7 at.% of Mg, they obtained the limit of the solubility of Cu in Mg<sub>2</sub>Ni at 25 at.%. In addition, isopleths with respectively constant X<sub>Cu</sub>/X<sub>Ni</sub> ratios of 2.0, 1.0 and 0.5 were constructed from differential thermal analysis, X-ray diffraction and isopiestic vapor pressure measurements [11, 13-16]. From the experimental data, the authors proposed the location of the monovariant reaction line on the liquidus surface and defined the four invariant equilibria: the ternary eutectic I<sub>1</sub> at 753 K (L ⇌ Mg<sub>2</sub>Ni + CuMg<sub>2</sub> + HCP) [11, 17], the four-phase reactions II<sub>1</sub> at 1081 K (L + MgNi<sub>2</sub> ⇌ FCC + Cu<sub>2</sub>Mg) [11, 10], II<sub>2</sub> at 931 K (L + MgNi<sub>2</sub> ⇌ Mg<sub>2</sub>Ni + Cu<sub>2</sub>Mg) [11, 17] and II<sub>3</sub> at 813 K (L + Cu<sub>2</sub>Mg ⇌ CuMg<sub>2</sub> + Mg<sub>2</sub>Ni) [11, 17].

#### *Thermodynamic data:*

T. Gnanasekaran et al. [13-16] determined the Mg activity at 1173 K over the Cu-Mg-Ni liquid alloys along three isopleths with X<sub>Cu</sub>/X<sub>Ni</sub> = 2.0, 1.0 and 0.5 from measurements of the Mg vapor pressures, using isopiestic method.

Feuler et al. [18] measured the integral enthalpy of mixing of the ternary liquid Cu-Mg-Ni alloy at 1008 K for the following compositions: Cu<sub>x</sub>Ni<sub>1-x</sub>-Mg, Mg<sub>x</sub>Ni<sub>1-x</sub>-Cu, Cu<sub>x</sub>Mg<sub>1-x</sub>-Ni, Cu<sub>x</sub>Mg<sub>1-x</sub>-Mg<sub>0.667</sub>Ni<sub>0.333</sub> and Cu<sub>x</sub>Ni<sub>1-x</sub>-Mg.

#### *Crystallographic data:*

Firauf [19] provided the first determination of the face-centered cubic C15-type crystal structure of the Cu<sub>2</sub>Mg phase, and the results were confirmed later by others studies [20-23].

Grime et al. [24] suggested that the crystal structure of Mg<sub>2</sub>Cu was hexagonal, but this result was revealed incorrect. Reevaluation indicated that the true unit cell is orthorhombic [20, 25].

The hexagonal C36-type structure of Ni<sub>2</sub>Mg was reported by numerous authors in the literature [9, 23, 26-28]. Laves and Witte [30] also determined the hexagonal C36-type structure of Ni<sub>2</sub>Mg and established the similarity of the C15 and C36-type structure.

Mg<sub>2</sub>Ni exhibits hexagonal C16-type structure as reported by Schubert et al. [25] and Raynor et al. [29].

### 3. Thermodynamic models

#### 3.1. Liquid, FCC-A1 and HCP-A3 solid solutions

The molar Gibbs energy of mixing is expressed by a sub-regular solution model using Muggianu's [31] formalism in which composition dependence is based on the Redlich-Kister equation. The molar Gibbs energy for a solution phase  $\phi$  is given by the formula:

$$G_m^\phi - H_m^{SER} = {}^{ref}G^\phi + {}^{id}G^\phi + {}^{xs}G^\phi \quad (1)$$

and

$${}^{ref}G^\phi = \sum_i x_i \left( {}^0G_i^\phi - H_i^{SER}(298.15K) \right) \quad (2)$$

$${}^{id}G^\phi = RT \sum_i x_i \ln(x_i) \quad (3)$$

$${}^{xs}G^\phi = \sum_i \sum_{j>i} x_i x_j \sum_{\nu=0}^n \left( {}^\nu L_{i,j}^\phi (x_i - x_j)^\nu \right) + x_{Cu} x_{Mg} x_{Ni} \sum_{\nu'=0}^2 \left( {}^{\nu'} L_{Cu,Mg,Ni}^\phi x_{\nu'} \right) \quad (4)$$

where  ${}^{ref}G^\phi$  is the contribution of the pure components,  ${}^{id}G^\phi$  is the ideal mixing contribution,  ${}^{xs}G^\phi$  is the contribution of the non-ideal interactions between the components;  $x_i$  is the mole fraction of the constituent  $i$  ( $i = Cu, Mg, Ni$ );  ${}^0G_i^\phi$  is the Gibbs energy of pure constituent  $i$  in the  $\phi$  state;  $H_i^{SER}$  is the enthalpy of pure constituent  $i$  in its stable state at  $T = 298.15$  K;  ${}^\nu L_{i,j}^\phi$  represents the binary interaction parameters dependant on the value of the Redlich-Kister coefficient  $\nu$  (0, 1, 2, ...), they are taken from the constituent binary system [2, 4-6];  ${}^{\nu'} L_{Cu,Mg,Ni}^\phi$  is the excess ternary interaction parameter, depending on the value of the coefficient  $\nu'$  (0, 1, 2: respectively for the contribution of Cu, Mg and Ni). It takes the following form:

$${}^{\nu'} L_{Cu,Mg,Ni}^\phi = a + b \cdot T \quad (5)$$

where  $a$  and  $b$  are constants to be evaluated for the solution phases Liquid and FCC-A1, from the experimental data. Ternary interaction in HCP-A3 is not considered in this assessment since the solubility of Cu and Ni in HCP Mg was reported to be negligible in the literature [11, 12].

### 3.2. Non-stoichiometric compounds:

The molar Gibbs energy of compounds exhibiting a homogeneity range is written as :

$$G_m^\phi - H^{SER} = {}^{ref}G^\phi + {}^{id}G^\phi + {}^{xs}G^\phi \quad (6)$$

where for a two sublattices model:

$${}^{id}G^\phi = RT \frac{1}{p+q} \left( p \sum_i {}^1y_i \ln({}^1y_i) + q \sum_i {}^2y_i \ln({}^2y_i) \right) \quad (7)$$

$${}^{ref}G^\phi = \frac{1}{p+q} \sum_i \sum_j {}^1y_i {}^2y_j {}^0G_{ij}^\phi \quad (8)$$

$${}^{xs}G^\phi = \frac{1}{p+q} \left( \sum_i \sum_{j>i} \sum_k {}^1y_i {}^1y_j {}^2y_k L_{i,j,k}^\phi + \sum_i \sum_j \sum_{k>j} {}^1y_i {}^2y_j {}^2y_k L_{i,j,k}^\phi \right) \quad (9)$$

$${}^0G_{ij}^\phi = p {}^0G_i^\phi + q {}^0G_j^\phi + a + b \cdot T \quad (10)$$

where  $i, j$  and  $k$  denote the elements (Cu, Mg, Ni) mixing on each sublattice (1 and 2);  ${}^1y_i$  and  ${}^2y_i$  are the fractional site occupancy of the element  $i$  on first and second sublattices respectively;  $p$  and  $q$  are the molar number of the sites in sublattice 1 and sublattice 2, respectively;  $L_{i,j,k}^\phi$  and  $L_{i,j,k}^\phi$  denote interaction parameters of mixing with the following form:

$$L_{i,j,k}^\phi = \sum_{\nu=0}^n \left( {}^\nu L_{i,j,k}^\phi (x_i - x_j)^\nu \right)$$

$${}^\nu L_{i,j,k}^\phi = a + b \cdot T$$

#### Mg<sub>2</sub>Cu and Laves-C16 Mg<sub>2</sub>Ni phases:

Mg<sub>2</sub>Cu and its extension in the ternary is described by the following sublattice model: (Mg)<sub>2</sub>(Cu,Ni). With this model the compound energy formalism has one member for the ideal compound and two for the hypothetical compounds. The parameter  $G_{Mg,Cu}^{Mg_2Cu} - 2 \cdot G_{Mg}^{HCP} - G_{Cu}^{FCC}$ , representing Mg<sub>2</sub>Cu in the binary system, is taken from the assessment by Buhler et al. [2, 4]. The parameter  $G_{Mg,Ni}^{Mg_2Cu}$  belongs to the hypothetical compound

Mg<sub>2</sub>Ni in the structure of Mg<sub>2</sub>Cu, together with  $L_{Mg,Cu,Ni}^{Mg_2Cu}$  describe the Mg<sub>2</sub>Cu phase along the section Mg<sub>2</sub>Cu-Mg<sub>2</sub>Ni.

Since not much phase diagram information is available for this phase, the parameter  $G_{Mg,Ni}^{Mg_2Cu}$  is expressed as a function of  $G_{Mg,Ni}^{L-C16}$  by adding a positive value:

$$G_{Mg,Ni}^{Mg_2Cu} = a + G_{Mg,Ni}^{L-C16}$$

The same treatment is applied to describe the Laves-C16 Mg<sub>2</sub>Ni phase, with the following sublattice model: (Mg)<sub>2</sub>(Cu,Ni). The parameter  $G_{Mg,Ni}^{L-C16}$  is accepted from the binary system [5].  $G_{Mg,Cu}^{L-C16} - 2 \cdot G_{Mg}^{HCP} - G_{Cu}^{FCC} = a + G_{Mg,Cu}^{Mg_2Cu}$  and  $L_{Mg,Cu,Ni}^{L-C16} = a + b \cdot T$  have to be evaluated from the experimental information.

#### Laves-C15 Cu<sub>2</sub>Mg and Laves-C36 Ni<sub>2</sub>Mg phases:

Because L-C15 and L-C36 phases are present in the Al-Cu-Mg ternary system, the possibility to include Al in their sublattice structure must be envisaged in order to extrapolate the present description to a higher order system, such as the Al-Cu-Mg-Ni quaternary system. It is why L-C15 and L-C36 phase modeling has been made consistent with the evaluation of the Al-Cu-Mg system done by Buhler et al. [2, 4]. The sublattice is described as follows: (Cu,Ni,Mg)<sub>2</sub>(Mg,Cu,Ni). The compound energy formalism has nine members for the ideal and hypothetical compounds, and eighteen interaction parameters.

The parameters  $G_{Ni,Mg}^{L-C15}$  and  $L_{Cu,Ni,Mg}^{L-C15}$  describe the Laves-C15 phase along the section Cu<sub>2</sub>Mg-Ni<sub>2</sub>Mg. They are adjusted to the available experimental data. The parameters  $G_{Ni,Mg}^{L-C15}$ , representing the Gibbs energy of the metastable phase Ni<sub>2</sub>Mg in the Laves-C15 structure, is expressed with the same function as  $G_{Ni,Mg}^{L-C36}$ , determined by Jacobs et al. [5], with the addition of a positive number. Also the interaction Cu-Ni was chosen to be linearly temperature dependent:

$$G_{Ni,Mg}^{L-C15} = a + G_{Ni,Mg}^{L-C36} \text{ and } L_{Cu,Ni,Mg}^{L-C15} = a + b \cdot T$$

All the others parameters are accepted from the literature or were fixed by assumption.

The parameters  $G_{Cu,Cu}^{L-C15} - 3 \cdot G_{Cu}^{FCC}$  and  $G_{Mg,Mg}^{L-C15} - 3 \cdot G_{Mg}^{HCP}$  describe the pure elements in the state of the Laves-C15 phase, and their values are accepted from Buhler et al. [2, 4]. The same value was assumed for  $G_{Ni,Ni}^{L-C15} - 3 \cdot G_{Ni}^{FCC}$ .

$G_{Cu,Ni}^{L-C15} - 2 \cdot G_{Cu}^{FCC} - G_{Ni}^{FCC}$  and  $G_{Ni,Cu}^{L-C15} - G_{Cu}^{FCC} - 2 \cdot G_{Ni}^{FCC}$  represent fictitious compounds Cu<sub>2</sub>Ni and Ni<sub>2</sub>Cu in the state of Laves-C15 phase, and since the atomic sizes of Cu and Ni are not very different, a value of 15000 J/mol is chosen for the parameters in analogy to the pure elements.

The parameters  $G_{Cu,Mg}^{L-C15}$  and  $G_{Mg,Cu}^{L-C15} - G_{Cu}^{FCC} - 2 \cdot G_{Mg}^{HCP}$  describe the Laves-C15 phase in the binary Cu-Mg and are accepted from the thermodynamic assessment of Buhler et al. [2, 4].

The parameters  $G_{Mg,Ni}^{L-C15}$  represent a highly hypothetical compound (antistructure atoms). In order to insure its insignificance, the approach previously used by Buhler et al. [2, 4] is applied: the Gibbs energy of the defects Ni antistructure atoms is  $G_{Ni,Ni}^{L-C15} - G_{Ni,Mg}^{L-C15}$ , and  $G_{Mg,Mg}^{L-C15} - G_{Ni,Mg}^{L-C15}$  for the defect Mg antistructure atoms, therefore:

$$G_{Mg,Ni}^{L-C15} = G_{Mg,Mg}^{L-C15} + G_{Ni,Ni}^{L-C15} - G_{Ni,Mg}^{L-C15}$$

The homogeneity range of the Cu<sub>2</sub>Mg phase in the binary is controlled by  $L_{Cu,Cu,Mg}^{L-C15}$  and  $L_{Cu,Mg,Mg}^{L-C15}$ . These parameters are accepted from Buhler et al. [2, 4].

The change of width of the homogeneity range of the Laves-C15 phase along the Cu<sub>2</sub>Mg-Ni<sub>2</sub>Mg section is modeled by the parameters  $L_{Ni,Mg,Ni}^{L-C15}$  and  $L_{Mg,Ni,Mg}^{L-C15}$ . Since no data are available in the literature, the adjustment

of these parameters is not possible and they are taken equal to those of the Laves-C36 Ni<sub>2</sub>Mg phase, which were optimized by Jacobs et al. [5].

All other interactions are less significant and are assumed independent of the occupation of the non-interacting site or expressed as a function of others:

$$L_{Cu,Ni:Cu}^{L-C15} = L_{Cu,Ni:Ni}^{L-C15} = a' + L_{Cu,Ni:Mg}^{L-C15} = a' + a + b T$$

and

$$L_{Cu:Cu,Mg}^{L-C15} = L_{Mg:Cu,Mg}^{L-C15} = L_{Ni:Cu,Mg}^{L-C15}$$

$$L_{Cu,Mg:Cu}^{L-C15} = L_{Cu,Mg:Mg}^{L-C15} = L_{Cu,Mg:Ni}^{L-C15}$$

$$L_{Cu:Mg,Ni}^{L-C15} = L_{Mg:Mg,Ni}^{L-C15} = L_{Ni:Mg,Ni}^{L-C15}$$

$$L_{Mg,Ni:Cu}^{L-C15} = L_{Mg,Ni:Mg}^{L-C15} = L_{Mg,Ni:Ni}^{L-C15}$$

Because of their relative unimportance and the fact that no assumptions could be made, the parameters  $L_{Cu:Cu,Ni}^{L-C15}$ ,  $L_{Mg:Cu,Ni}^{L-C15}$  and  $L_{Ni:Cu,Ni}^{L-C15}$  were ignored and fixed equal to zero.

The same treatment is performed for the Laves-C36 Ni<sub>2</sub>Mg phase, with the sublattice model: (Cu,Mg,Ni)<sub>2</sub>(Cu,Mg,Ni). The following parameters are adopted from the literature:

$$G_{Ni:Mg}^{L-C36}, G_{Mg:Ni}^{L-C36}, G_{Mg:Mg}^{L-C36}, G_{Ni:Ni}^{L-C36} \quad [5]$$

$$L_{Mg:Mg,Ni}^{L-C36}, L_{Ni:Mg,Ni}^{L-C36}, L_{Mg,Ni:Mg}^{L-C36}, L_{Mg,Ni:Ni}^{L-C36} \quad [5]$$

$$G_{Cu:Mg}^{L-C36}, G_{Mg:Cu}^{L-C36}, G_{Cu:Cu}^{L-C36} \quad [2, 4]$$

$$L_{Cu:Cu,Mg}^{L-C36}, L_{Mg:Cu,Mg}^{L-C36}, L_{Cu,Mg:Cu}^{L-C36}, L_{Cu,Mg:Mg}^{L-C36} \quad [2, 4]$$

and the following parameters are fixed by making the same assumption as above:

$$L_{Cu:Cu,Mg}^{L-C36} = L_{Mg:Cu,Mg}^{L-C36} = L_{Ni:Cu,Mg}^{L-C36}$$

$$L_{Cu,Mg:Cu}^{L-C36} = L_{Cu,Mg:Mg}^{L-C36} = L_{Cu,Mg:Ni}^{L-C36}$$

$$L_{Cu:Mg,Ni}^{L-C36} = L_{Mg:Mg,Ni}^{L-C36} = L_{Ni:Mg,Ni}^{L-C36}$$

$$L_{Mg,Ni:Cu}^{L-C36} = L_{Mg,Ni:Mg}^{L-C36} = L_{Mg,Ni:Ni}^{L-C36}$$

For the L-C36 Ni<sub>2</sub>Mg phase, only  $L_{Cu,Ni:Mg}^{L-C36}$ ,  $L_{Cu,Ni:Cu}^{L-C36}$  and  $L_{Cu,Ni:Ni}^{L-C36}$  have to be evaluated from the experimental data:

$$L_{Cu,Ni:Cu}^{L-C36} = L_{Cu,Ni:Ni}^{L-C36} = a' + L_{Cu,Ni:Mg}^{L-C36} = a' + a + b.T$$

In the next section the procedure for evaluation of the parameters a, a' and b of the previous expression of G and L is presented.

#### 4. Evaluation of the thermodynamic parameters:

All the experimental results selected to evaluate the parameters of the thermodynamic models for the Gibbs energy of individual phases are summarized in Tables 1-4. The parameters were evaluated using the PARROT [32] module in Thermocalc [33]. This software allows the introduction of a great variety of experimental data in the optimization. The program works by minimizing the square of error sum between calculated and experimental data values.

The parameters representing the ternary interaction in the liquid phase are optimized first, by fitting Mg activity and enthalpy of mixing measurements [13-18]. Given that no ternary compounds are present in this system, the model parameters for the other phases are evaluated by sequence, starting with the Cu-Cu<sub>2</sub>Mg-Ni<sub>2</sub>Mg-Ni region. The parameters of the L-C15, L-C36 and FCC phases are manually adjusted and then optimized according to the experimental data selected for this region. The thermodynamic description of the L-

C16 and Cu<sub>2</sub>Mg phases are developed by fitting the experimental data selected in the region Cu<sub>2</sub>Mg-Mg-Ni<sub>2</sub>Mg. Due to the lack of experimental data, some parameters have to be manually readjusted after optimization in order to improve the overall agreement between calculated and experimental data values.

### 5. Results and discussion:

The parameters evaluated in the present description of the Cu-Mg-Ni system are listed in the appendix. The thermodynamic description of the three pure elements (Cu, Mg, Ni) are taken from Dinsdale [34]. Figure 4 illustrates the liquidus projection and the monovariant reaction line calculated using the present evaluation. In the same figure, measurements by Fehrenback et al. [10] of the monovariant eutectic trough, extending between the binary eutectic Cu-Cu<sub>2</sub>Mg and Ni-Ni<sub>2</sub>Mg, are plotted. A deviation between calculated and measured values is apparent when Ni concentration increases. This could be because higher weight was given to the data concerning the Mg activity and mixing enthalpy in the liquid, assumed to be more reliable. It can be seen, from Figs. 5-10, that the various measured Mg activities and enthalpy of mixing in the liquid are reproduced with reasonable agreement. The values of the ternary interaction parameters of the liquid phase indicate an unequal contribution of each element. With an attractive contribution of Mg and repulsive for Cu and Ni, the iso-Gibbs energy curves for the liquid Cu-Mg-Ni alloys must be shifted to the Mg-rich corner. Similar asymmetry was previously noticed by Gnanasekara et al. [15]; using the formalism of Bonnier and Gaboz [35], they found comparable results as those above in terms of the sign of each contribution.

The calculated temperatures and compositions of the phases at the invariant reactions are listed and compared to the experimental data in Table 4. Reasonably good agreement is obtained for the calculated temperatures as well as for the compositions. The reaction sequence elaborated by Fehrenbach et al. [10] is well reproduced. If the match is almost perfect for the class I reaction, the calculated liquid composition differs by a maximum of 20% for the Mg and Cu concentration at the reactions II<sub>1</sub>, II<sub>2</sub> and II<sub>3</sub>, according the compilation by Chang et al. [17]. However, since 1956 no study was performed to confirm or improve the estimation by Mikheeva et al. [8].

Calculated isopleths for X(Cu)/X(Ni) = 2, 1 and 0.5 are shown in Figs. 11-13. Good agreement is observed between calculated liquidus temperatures and experimental data. Furthermore most of the experimental points, such as phase field limits and invariant reactions, are reasonably reproduced. However, the calculated liquidus for X(Mg) = 0.71 (Fig. 14) presents an unexpected shoulder up to 10 % Mg (mole fraction), and the L-C36 and L-C15 phases, when extended in the ternary description (Fig. 11-13), appear to be less stable at high temperature than indicated by Ipser et al. [11].

According to Ipser et al. [11] the phase field (L-C36 + L-C16) shows up in the isopleth section at X(Cu)/X(Ni) = 1, confirming the results compiled by Chang et al. [17] that the L-C36 phase is in equilibrium at 931 K with the L-C16 phase containing up to 21 % Cu (mole fraction). Given the work of Buhler et al. [2, 4] and Jacobs et al. [5], only one significant parameter can be adjusted in the present work for the L-C36 phase:  ${}^0L_{Cu,NiMg}^{L-C36}$ . Since the ternary solubility of L-C36 is well established, the window to adjust this parameter is narrow. The problem is similar for the L-C16 phase for which only two adjustable parameters are available. In order to respect the above experimental results, a sub-regular term  ${}^1L_{Mg,Cu,Ni}^{L-C16}$  has to be introduced, allowing to stretch the phase field (L-C36 + L-C16) up to 17.3 at.% Cu in the L-C16 phase around 900 K. But by doing this, the agreement with the experimental liquidus temperature data at X(Mg) = 0.71 is deteriorated. This choice was made since only few experimental compositions were investigated on the liquidus [11] and because the temperature and composition were not given in the original publication, but had to be read out from the figure, which introduces a significant uncertainty.

For the L-C36 phase, as indicated above, only one adjustable parameter remains to reproduce two properties: its stability at high temperature and its ternary solubility. Since the latter property is well reported to

be small by several authors [10, 11], more importance was given to it, which explains the lack of stability of L-C36 at high temperature.

For the L-C15 phase, the problem is to obtain the important ternary solubility [10, 11] and, at the same time, to narrow the phase field in which it is involved with the FCC phase [10]. Indeed, based on the analyses of two alloy compositions (35 at.% Ni, 48 Cu, 17 Mg, and 46 at.% Ni, 39 Cu, 15 Mg,) homogenized at 1073 K, Fehrenbach et al. [10] fixed the corners of the three-phase triangle involving L-C15, L-C36 and FCC. Considering these measurements very reliable, great importance was attached to reproduce them. In order to maintain both above alloys in the ternary triangle and to allow significant solubility of Ni in L-C15 (Fig. 15), the stability of the L-C15 phase has to be limited, even with the introduction of a sub-regular parameter for the Cu-Ni interaction in the first sublattice.

Calculated isothermal sections at 1073 K and 673 K are presented in Figs. 15 and 16 respectively. It can be seen that the ternary solubility of the L-C16, Mg<sub>2</sub>Cu, L-C15 and L-C36 phases is well reproduced, as well as the location of the ternary phase triangle proposed by Fehrenbach and al. [10] and Karonik and al. [12].

### 6. Summary:

A self-consistent thermodynamic description for the complete Cu-Mg-Ni ternary system is presented. The Laves phases are evaluated based on the work done by Buhler et al. [2, 4], insuring a total compatibility with their description of the Al-Cu-Mg system in order to extrapolate the present description to the Al-Cu-Mg-Ni system. Overall reasonable agreement is obtained between calculated and available experimental data. Calculated ternary solubility of the binary compounds is satisfactorily reproduced, as well as Mg activity and enthalpy of mixing in the liquid phase. Various isoplethal and isothermal sections are calculated and demonstrate good consistency with the literature. However, further experimental data are necessary in order to obtain a more reliable thermodynamic description of the Cu-Mg-Ni system.

### Acknowledgments

SG gratefully acknowledges Dr D.B. Miracle and support of this research by the Air Force Research Laboratory under Contract No. F33615-99-C-5803. GJS acknowledges support from the National Science Foundation under grant DMR-9972941. The authors wish to thank Dr. Liu Zi-Kui for discussions.

### Appendix

Thermodynamic parameters for the Cu-Mg-Ni system.

\*: indicates coefficient evaluated in the present work.

\*\* : indicates coefficient fixed by assumption.

Liquid, sublattice model: (Cu,Mg,Ni)

$${}^0L_{\text{Cu,Mg}}^{\text{Liq}} = -36984 + 4.75612 \cdot T \quad [2, 4]$$

$${}^1L_{\text{Cu,Mg}}^{\text{Liq}} = -8191.29 \quad [2, 4]$$

$${}^0L_{\text{Cu,Ni}}^{\text{Liq}} = 11760 + 1.084 \cdot T \quad [6]$$

$${}^1L_{\text{Cu,Ni}}^{\text{Liq}} = -1671.8 \quad [6]$$

$${}^0L_{\text{Mg,Ni}}^{\text{Liq}} = -50910 + 25.79995 \cdot T \quad [5]$$

$${}^1L_{\text{Mg,Ni}}^{\text{Liq}} = -14989.95 + 1324788 \cdot T \quad [5]$$

$${}^0L_{\text{Cu,Mg,Ni}}^{\text{Liq}} = 15000 \quad *$$



$${}^1 L_{\text{Cu,Mg,Ni}}^{\text{Liq}} = -25000 \quad *$$

$${}^2 L_{\text{Cu,Mg,Ni}}^{\text{Liq}} = 10000 \quad *$$

FCC-A1, sublattice model: (Cu,Mg,Ni)(Va)

$${}^0 L_{\text{Cu,Mg,Va}}^{\text{FCC}} = -22279.28 + 5.868 \cdot T \quad [2, 4]$$

$${}^0 L_{\text{Cu,Ni,Va}}^{\text{FCC}} = 8366 + 2.802 \cdot T \quad [6]$$

$${}^1 L_{\text{Cu,Ni,Va}}^{\text{FCC}} = -4359.6 + 1.812 \cdot T \quad [6]$$

$${}^0 L_{\text{Mg,Ni,Va}}^{\text{FCC}} = 50000 \quad [5]$$

$${}^0 L_{\text{Cu,Mg,Ni,Va}}^{\text{FCC}} = -30000 \quad *$$

$${}^1 L_{\text{Cu,Mg,Ni,Va}}^{\text{FCC}} = 10000 \quad *$$

$${}^2 L_{\text{Cu,Mg,Ni,Va}}^{\text{FCC}} = -130000 \quad *$$

HCP-A3, sublattice model: (Cu,Mg,Ni)(Va)<sub>1/2</sub>

$${}^0 L_{\text{Cu,Ni,Va}}^{\text{HCP}} = 8366 + 2.802 \cdot T \quad [6]$$

$${}^0 L_{\text{Mg,Ni,Va}}^{\text{HCP}} = 50000 \quad [5]$$

Mg<sub>2</sub>Cu phase, sublattice model: (Mg)<sub>2</sub>(Cu,Ni)

$$G_{\text{Mg,Cu}}^{\text{Mg}_2\text{Cu}} - 2 \cdot G_{\text{Mg}}^{\text{HCP}} - G_{\text{Cu}}^{\text{FCC}} = -28620 + 1.85973 \cdot T \quad [2, 4]$$

$$G_{\text{Mg,Ni}}^{\text{Mg}_2\text{Cu}} = -55691.2 + 415.47933 \cdot T - 74.8062 \cdot T \cdot \ln T - 4.6155 \cdot 10^{-3} \cdot T^2 + 401415 \cdot T^{-1} \quad *$$

$${}^0 L_{\text{Mg,Cu,Ni}}^{\text{Mg}_2\text{Cu}} = -25000 + 36.28 \cdot T \quad *$$

Laves C-16 Mg<sub>2</sub>Ni(Cu) phase, sublattice model: (Mg)<sub>2</sub>(Cu,Ni)

$$G_{\text{Mg,Ni}}^{\text{L-C16}} = -60961.2 + 415.47933 \cdot T - 74.8062 \cdot T \cdot \ln T - 4.6155 \cdot 10^{-3} \cdot T^2 + 401415 \cdot T^{-1} \quad [5]$$

$$G_{\text{Mg,Cu}}^{\text{L-C16}} - 2 \cdot G_{\text{Mg}}^{\text{HCP}} - G_{\text{Cu}}^{\text{FCC}} = -23720 + 1.85973 \cdot T \quad *$$

$${}^0 L_{\text{Mg,Cu,Ni}}^{\text{L-C16}} = -10000 - 4.3 \cdot T \quad *$$

$${}^1 L_{\text{Mg,Cu,Ni}}^{\text{L-C16}} = -17800 \quad *$$

Laves C-15 Cu<sub>2</sub>Mg phase, sublattice model: (Cu,Mg,Ni)<sub>2</sub>(Cu,Mg,Ni)

$$G_{\text{Cu,Cu}}^{\text{L-C15}} - 3 \cdot G_{\text{Cu}}^{\text{FCC}} = 15000 \quad [2, 4]$$

$$G_{\text{Mg,Mg}}^{\text{L-C15}} - 3 \cdot G_{\text{Mg}}^{\text{HCP}} = 15000 \quad [2, 4]$$

$$G_{\text{Ni,Ni}}^{\text{L-C15}} - 3 \cdot G_{\text{Ni}}^{\text{FCC}} = 15000 \quad **$$

$$G_{\text{Cu,Mg}}^{\text{L-C15}} = -54690.99 + 364.73085 \cdot T - 69.276417 \cdot T \cdot \ln T - 5.19246 \cdot 10^{-4} \cdot T^2 + 143502 \cdot T^{-1} - 5.65953 \cdot 10^{-6} \cdot T^3 \quad [2, 4]$$

$$G_{\text{Mg,Cu}}^{\text{L-C15}} - 2 \cdot G_{\text{Mg}}^{\text{HCP}} - G_{\text{Cu}}^{\text{FCC}} = 104970.96 - 16.46448 \cdot T \quad [2, 4]$$

$$G_{\text{Cu,Ni}}^{\text{L-C15}} - 2 \cdot G_{\text{Cu}}^{\text{FCC}} - G_{\text{Ni}}^{\text{FCC}} = 15000 \quad **$$

$$G_{\text{Ni,Cu}}^{\text{L-C15}} - G_{\text{Cu}}^{\text{FCC}} - 2 \cdot G_{\text{Ni}}^{\text{FCC}} = 15000 \quad **$$

$$G_{\text{Ni,Mg}}^{\text{L-C15}} = 60165.38 + 441.81039 \cdot T - 77.394 \cdot T \cdot \ln T - 7.39488 \cdot 10^{-3} \cdot T^2 + 334726.5 \cdot T^{-1} \quad *$$

$$G_{\text{Mg,Ni}}^{\text{L-C15}} = G_{\text{Mg,Mg}}^{\text{L-C15}} + G_{\text{Ni,Ni}}^{\text{L-C15}} - G_{\text{Ni,Mg}}^{\text{L-C15}} \quad *$$

$${}^0 L_{\text{Cu,Mg,Cu}}^{\text{L-C15}} = 13011.35 \quad [2, 4]$$

${}^0L_{Cu,Mg:Mg}^{L-C15} = 13011.35$	[2, 4]
${}^0L_{Cu,Mg:Ni}^{L-C15} = 13011.35$	**
${}^0L_{Cu:Cu,Mg}^{L-C15} = 6599.45$	[2, 4]
${}^0L_{Mg:Cu,Mg}^{L-C15} = 6599.45$	[2, 4]
${}^0L_{Ni:Cu,Mg}^{L-C15} = 6599.45$	**
${}^0L_{Mg,Ni:Cu}^{L-C15} = -10040.39007 + 59.88549 \cdot T$	**
${}^0L_{Mg,Ni:Mg}^{L-C15} = -10040.39007 + 59.88549 \cdot T$	**
${}^0L_{Mg,Ni:Ni}^{L-C15} = -10040.39007 + 59.88549 \cdot T$	**
${}^0L_{Cu:Mg,Ni}^{L-C15} = 30300$	**
${}^0L_{Cu:Mg,Ni}^{L-C15} = 30300$	**
${}^0L_{Cu:Mg,Ni}^{L-C15} = 30300$	**
${}^0L_{Cu,Ni:Mg}^{L-C15} = -34150 + 17.5 \cdot T$	*
${}^1L_{Cu,Ni:Mg}^{L-C15} = 8000$	*
${}^0L_{Cu,Ni:Cu}^{L-C15} = {}^0L_{Cu,Ni:Ni}^{L-C15} = 4850 + 17.5 \cdot T$	*

Laves C-36 Ni<sub>2</sub>Mg phase, sublattice model: (Cu,Mg,Ni)<sub>2</sub>(Cu,Mg,Ni)

$G_{Cu:Cu}^{L-C36} - 3 \cdot G_{Cu}^{FCC} = 15000$	[2, 4]
$G_{Mg:Mg}^{L-C36} - 3 \cdot G_{Mg}^{HCP} = 15000$	[2, 4]
$G_{Ni:Ni}^{L-C36} - 3 \cdot G_{Ni}^{FCC} = 15000$	[5]
$G_{Cu:Mg}^{L-C36} = -34690.99 + 364.73085 \cdot T - 69.276417 \cdot T \cdot \ln T - 5.19246 \cdot 10^{-4} \cdot T^2$ $+ 143502 \cdot T^{-1} - 5.65953 \cdot 10^{-6} \cdot T^3$	[2, 4]
$G_{Mg:Cu}^{L-C36} - 2 \cdot G_{Mg}^{HCP} - G_{Cu}^{FCC} = 84970.96 - 16.46448 \cdot T$	[2, 4]
$G_{Cu:Ni}^{L-C36} - 2 \cdot G_{Cu}^{FCC} - G_{Ni}^{FCC} = 15000$	**
$G_{Ni:Cu}^{L-C36} - G_{Cu}^{FCC} - 2 \cdot G_{Ni}^{FCC} = 15000$	**
$G_{Ni:Mg}^{L-C36} = -74065.38 + 441.81039 \cdot T - 77.3994 \cdot T \cdot \ln T - 7.39488 \cdot 10^{-3} \cdot T^2 + 334726.5 \cdot T^{-1}$	[5]
$G_{Mg:Ni}^{L-C36} - 2 \cdot G_{Mg}^{HCP} - G_{Ni}^{FCC} = 3000$	[5]
${}^0L_{Cu,Mg:Cu}^{L-C36} = 13011.35$	[2, 4]
${}^0L_{Cu,Mg:Mg}^{L-C36} = 13011.35$	[2, 4]
${}^0L_{Cu,Mg:Ni}^{L-C36} = 13011.35$	**
${}^0L_{Cu:Cu,Mg}^{L-C36} = 6599.45$	[2, 4]
${}^0L_{Mg:Cu,Mg}^{L-C36} = 6599.45$	[2, 4]
${}^0L_{Ni:Cu,Mg}^{L-C36} = 6599.45$	**
${}^0L_{Mg,Ni:Cu}^{L-C36} = -10040.39007 + 59.88549 \cdot T$	**
${}^0L_{Mg,Ni:Mg}^{L-C36} = -10040.39007 + 59.88549 \cdot T$	[5]
${}^0L_{Mg,Ni:Ni}^{L-C36} = -10040.39007 + 59.88549 \cdot T$	[5]
${}^0L_{Cu:Mg,Ni}^{L-C36} = 30300$	**

$${}^0L_{\text{Mg:Mg:Ni}}^{\text{L-C36}} = 30300 \quad [5]$$

$${}^0L_{\text{Ni:Mg:Ni}}^{\text{L-C36}} = 30300 \quad [5]$$

$${}^0L_{\text{Cu:Ni:Mg}}^{\text{L-C36}} = -78000 + 22.0 \cdot T \quad *$$

$${}^0L_{\text{Cu:Ni:Cu}}^{\text{L-C36}} = {}^0L_{\text{Cu:Ni:Ni}}^{\text{L-C15}} = 48035 + 22.0 \cdot T \quad *$$

### References

1. F. Q. Guo, S. J. Enouf, S. J. Poon and G. J. Shiflet, *Phil. Mag. Let.*, 81(3), 2001, 203-211.
2. T. Buhler, S. G. Fries, P. J. Spencer and H. L. Lukas, *J. Phase Equilibria*, 19(4), 1998, 315-333.
3. C. A. Coughanowr, I. Ansara, R. Luoma, M. Hamalainen and H. L. Lukas, *Z. Metallkd.*, 82, 1991, 574-581.
4. T. Buhler, unpublished work, 2001.
5. M. H. G. Jacobs and P. J. Spencer, *CALPHAD*, 22(4), 1998, 513-525.
6. A. Jansson, *TRITA-MAC*, 340, 1987.
7. W. Koster, *Z. Metallkd.*, 42, 1951, 326-327.
8. V. I. Mikheeva and G. G. Babayan, *Dokl. Akad. Nauk SSSR*, 108, 1956, 1086.
9. K. H. Lieser and H. Witte, *Z. Metallkd.*, 43, 1952, 396-401.
10. P. J. Fehrenbach, H. W. Kerr and P. Niessen, *J. Mater. Sci.*, 7, 1972, 1168-1174.
11. H. Ipser, T. Gnanasekaran, S. Boser and H. Mikler, *J. Alloys Compd.*, 227, 1995, 186-192.
12. V. V. Karonik, V. V. Guseva, A. V. Ivanishchev and V. E. Kolesnichenko, *Izv. Akad. Nauk SSSR, Met.*, 5, 1983, 182-186.
13. T. Gnanasekaran and H. Ipser, *J. Chim. Phys.*, 90, 1993, 367-372.
14. T. Gnanasekaran and H. Ipser, *J. Non-Cryst. Solids*, 156-158, 1993, 384-387.
15. T. Gnanasekaran and H. Ipser, *Metall. Trans.*, 25B, 1994, 63-72.
16. M. H. G. Jacobs, P. J. Spencer, *J. Alloys Compd.*, 220, 1995, 15-18.
17. Y. A. Chang, J. P. Neumann, A. Mikula and D. Goldberg, *The Metallurgy of Copper: Phase Diagrams and Thermodynamic Properties of Ternary Copper-Metal Systems*, INCRA Monograph VI, International Copper Research Association, Inc., 1979, 513.
18. H. Feufel and F. Sommer, *J. Alloys Compd.*, 224, (1995), 42-54.
19. J. B. Firauf, *J. Am. Chem. Soc.*, 49, 1927, 3107-3114.
20. A. Runqvist, H. Arnfelt and A. Westgren, *Z. Anorg. Chem.*, 175, 1928, 43-48.
21. T. Ohba, Y. Kitano and Y. Komura, *Acta Cryst. C*, 40(1), 1984, 1-5.
22. V. G. Sederman, *Phil. Mag.*, 18, 1934, 343-352.
23. P. Bagnoud and P. Feschotte, *Z. Metallkd.*, 69, 1978, 114-120.
24. G. Grime and W. Morris-Jones, *Philos. Mag.*, 7, 1929, 1113-1134.
25. K. Schubert and K. Anderko, *Z. Metallkd.*, 42, 1951, 321-325.
26. E. F. Bachmetew, *Metallwirtschaft*, 14, 1935, 1001-1002.
27. Y. Komura, A. Nakae and M. Mitarai, *Acta Cryst.*, B28, 1972, 727-732.
28. K. H. J. Buschow, *Solid State Commun.*, 17, 1975, 891-893.
29. G. V. Raynor. *The Physical Metallurgy of Magnesium and its Alloys*, Pergamon Press, Elmsford, NY, 1959.
30. F. Laves and H. Witte, *Metallwirtschaft*, 15, 1936, 15-22.
31. Y.-M. Muggiani, M. Gambino and J.-P. Bros, *J. Chim. Phys.*, 72, 1975, 83.
32. B. Jansson: *Trita-Mac-558, Evaluation of Parameters in Thermo-chemical Models Using Different Types of Experimental Data Simultaneously*, Royal Institute of Technology, Stockholm, 1984.
33. B. Sundman, B. Jansson, and J.-O. Anderson: *CALPHAD*, 9, 1985, 153.
34. A. T. Dinsdale: *CALPHAD*, 15, 1991, 317.
35. E. Bonnier and R. Caboz: *Compt. Rend.*, 250, 1960, 527-529.

Table 1: Summary of phase diagram investigations

	Composition region	T (K)	Ref.
5 experimental assessed isothermal sections	Cu-Cu <sub>2</sub> Mg-Ni <sub>2</sub> Mg-Ni region	1003, 1073, 1081 and 1123	10
	Mg-Mg <sub>2</sub> Cu-Mg <sub>2</sub> Ni	673	12
4 experimental assessed isopleths	X <sub>Cu</sub> /X <sub>Ni</sub> =2.0, 1.0 and 0.5, and X <sub>Mg</sub> =0.71	673 - 1400	11, 16
1 experimental quasibinary (only the liquidus)	Cu <sub>2</sub> Mg - Ni <sub>2</sub> Mg	1000 - 1450	9
1 eutectic trough extended from the binary Cu-Cu <sub>2</sub> Mg	Up to 25 at.% Ni	1001 - 1121	10

Table 2: Summary of experimental thermodynamic data

Quantity measured	Phase	Experimental method	T (K)	Composition	Ref.
Mg activity	Liquid	Isopiestic (Mg vapor pressure)	1173	Whole range of composition for 3 isopleths X <sub>Cu</sub> /X <sub>Ni</sub> =2.0, 1.0 and 0.5	13, 14, 15, 16
Integral enthalpy of mixing	Liquid	DSC	1008	Whole range of composition for Cu <sub>x</sub> Ni <sub>1-x</sub> -Mg, Mg <sub>x</sub> Ni <sub>1-x</sub> -Cu, Cu <sub>x</sub> Mg <sub>1-x</sub> -Ni, Cu <sub>x</sub> Mg <sub>1-x</sub> -Mg <sub>0.667</sub> Ni <sub>0.333</sub> and Cu <sub>x</sub> Ni <sub>1-x</sub> -Mg.	18

Table 3: Crystallographic structure and ternary solubility of the binary phases in the Cu-Mg-Ni system

Phase	Crystallography Structure Space / Group	Ref.	T (K)	Solubility Range	Ref.
Mg <sub>2</sub> Cu	Orthorhombic / Fddd	20, 25	540	1 at.% Ni	11
			673	< 2 at.% Ni	12
Mg <sub>2</sub> Ni	Hexagonal C16 / P6 <sub>2</sub> 22	25, 29	673	25 at.% Cu	12
			723	25 at.% Cu	11
			813	> 22 at.% Cu	11
Cu <sub>2</sub> Mg	FCC C15 / Fd3m	20-23	above 700	> 22 at.% Ni	11
			973	20 at.% Ni	10
Ni <sub>2</sub> Mg	Hexagonal C36 / P6 <sub>3</sub> /mmc	9, 23 26-28	931 - 1203	5 at.% Cu	11
			1073	3 - 7 at.% Cu	10

Table 4: Invariant liquidus reactions.

Class	Phases	Experiments					Present Calculation			
		T(K)	Composition at.%			Ref.	T(K)	Composition at.%		
			Cu	Mg	Ni			Cu	Mg	Ni
I <sub>1</sub>	Liquid	753	15	84	1	11, 17	760.1	15.4	83.7	0.9
	HCP		0	100	0			0	100	0
	Mg <sub>2</sub> Ni (L-C16)		25	67	8			24.8	66.7	8.5
	Mg <sub>2</sub> Cu		32	67	1			32.5	66.7	0.8
II <sub>1</sub>	Liquid	1081	65	20	15	11, 10	1106	58.9	24.6	16.5
	Cu <sub>2</sub> Mg (L-C15)		45	32	23			42.0	31.4	26.6
	Ni <sub>2</sub> Mg (L-C36)		5	32	63			7.8	32.3	59.9
	FCC		72	5	23			51.6	3.6	44.8
II <sub>2</sub>	Liquid	931	25	67	8	11, 17	932.8	31.9	57.1	11.0
	Ni <sub>2</sub> Mg (L-C36)		5	34	61			7.5	33.6	58.9
	Mg <sub>2</sub> Ni (L-C16)		21	67	12			17.3	66.7	16.0
	Cu <sub>2</sub> Mg (L-C15)		41	34	25			41.8	34.2	24.0
II <sub>3</sub>	Liquid	813	29	68	3	11, 17	826.0	39.7	59.7	0.6
	Cu <sub>2</sub> Mg (L-C15)		65	35	0			63.4	35.7	0.9
	Mg <sub>2</sub> Ni (L-C16)		25	67	8			25.0	66.7	8.3
	Mg <sub>2</sub> Cu		32	67	1			32.7	66.7	0.6

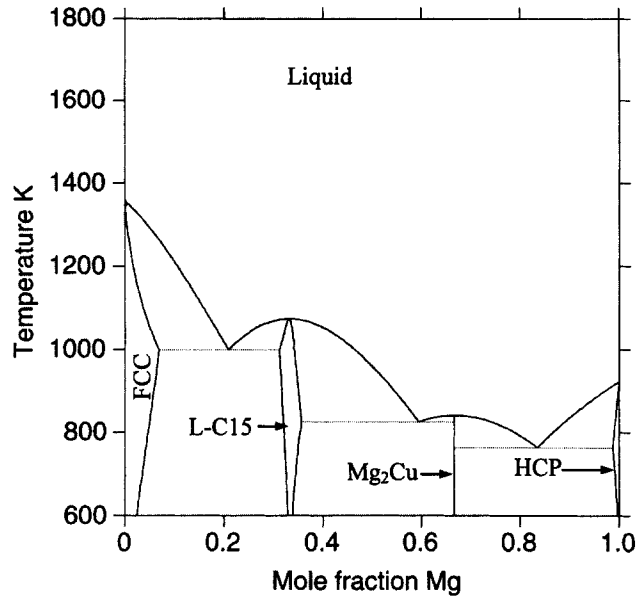


Figure 1: The Cu-Mg phase diagram calculated from the thermodynamic description by Buhler et al. [2, 4].

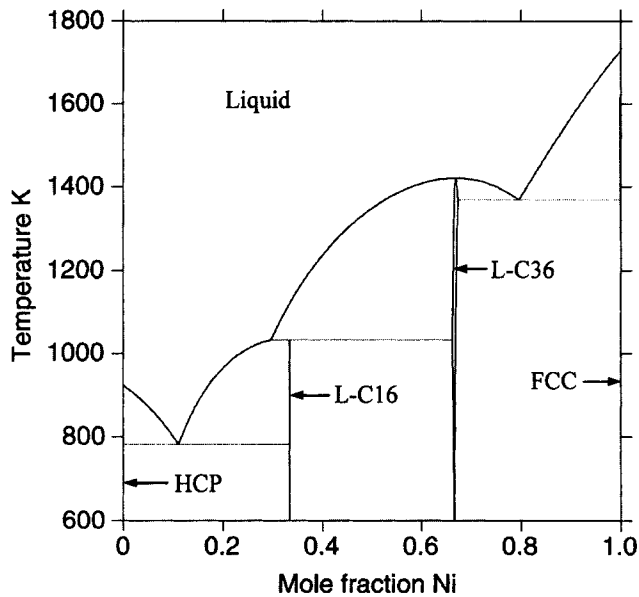


Figure 2: The Mg-Ni phase diagram calculated from the thermodynamic description by Jacobs et al. [5].

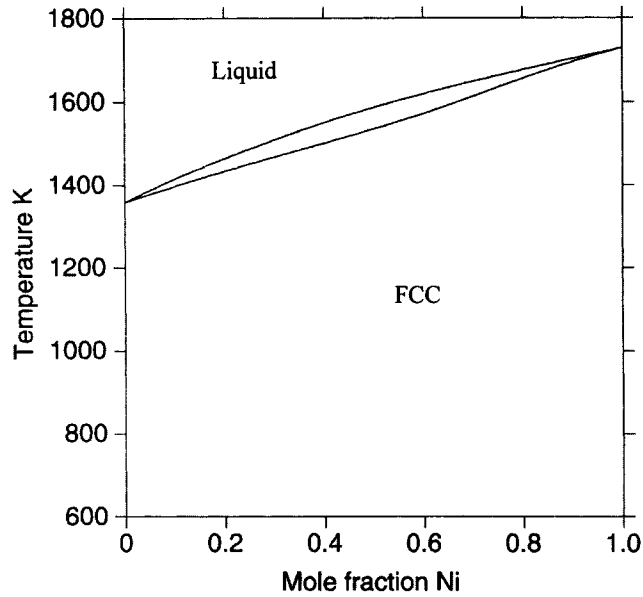


Figure 3: The Cu-Ni phase diagram calculated from the thermodynamic description by Jansson [6].

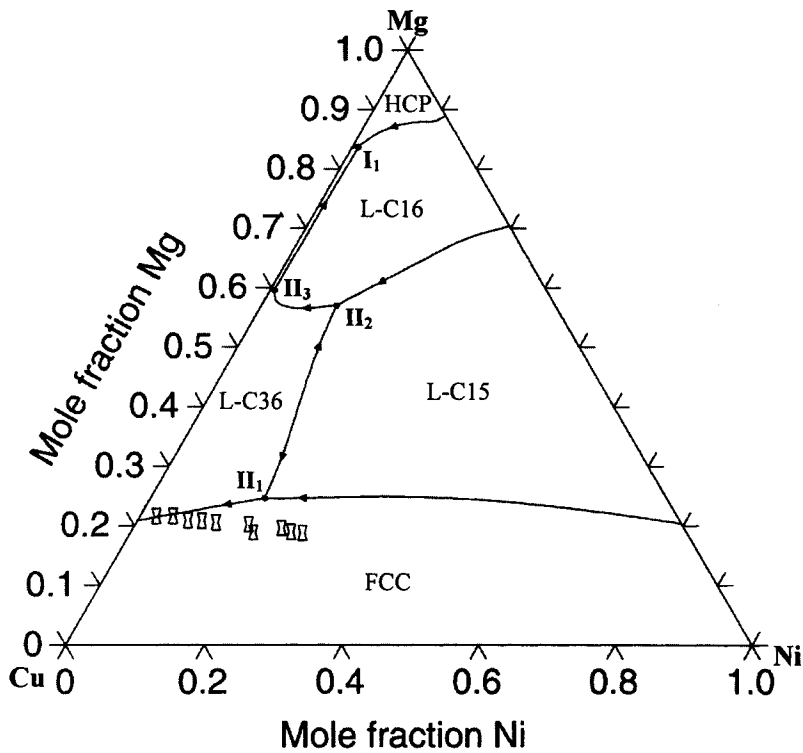


Figure 4: Calculated liquidus projection with symbols representing the composition of the experimental [10] monovariant eutectic trough extending between the binary eutectic Cu-Cu<sub>2</sub>Mg and Ni-Ni<sub>2</sub>Mg.

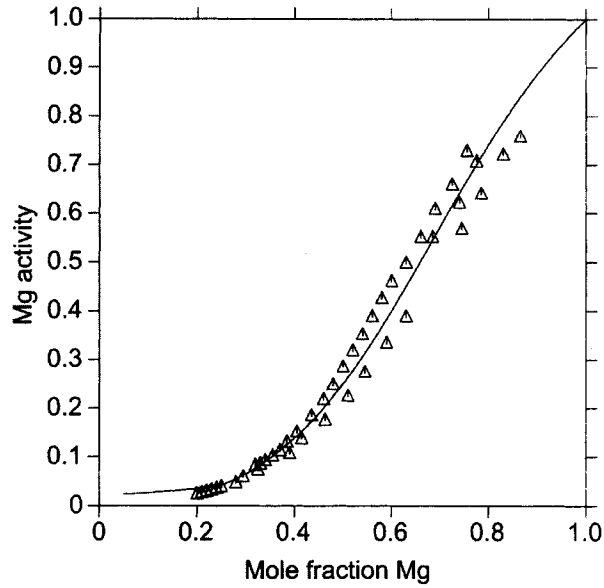


Figure 5: Mg activity at 1173 K for  $X(\text{Cu})/X(\text{Ni})=2$  according to the present description, compared with the experimental data from the literature [13-16].

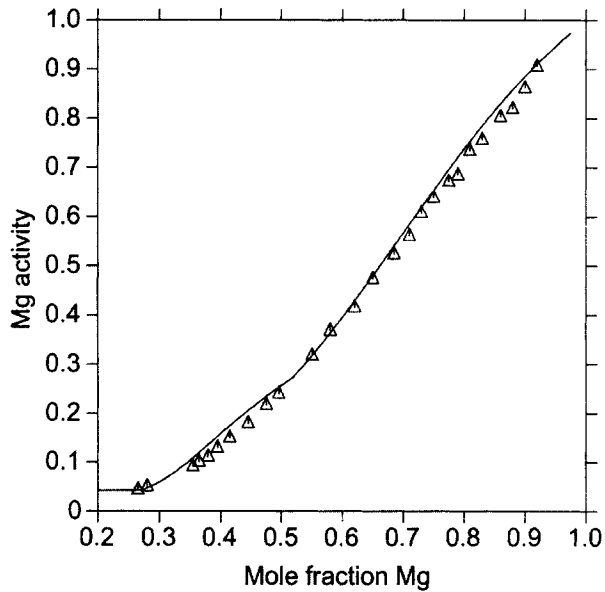


Figure 6: Mg activity at 1173 K for  $X(\text{Cu})/X(\text{Ni})=1$  according to the present description, compared with the experimental data from the literature [13-16].



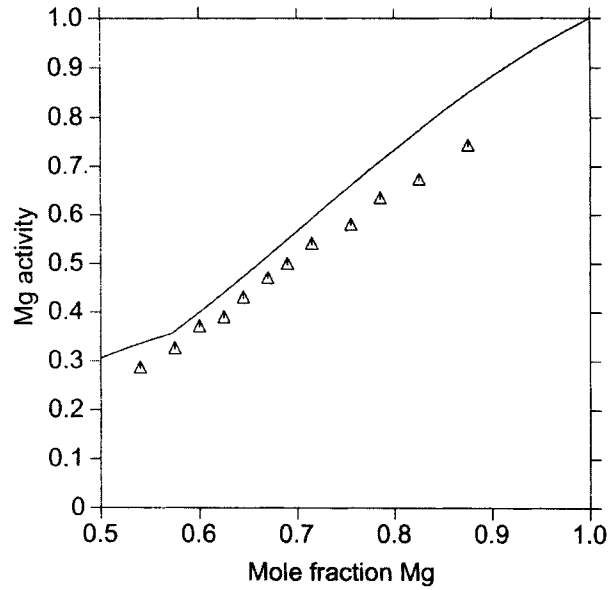


Figure 7: Mg activity at 1173 K for  $X(\text{Cu})/X(\text{Ni})=0.5$  according to the present description, compared with the experimental data from the literature [13-16].

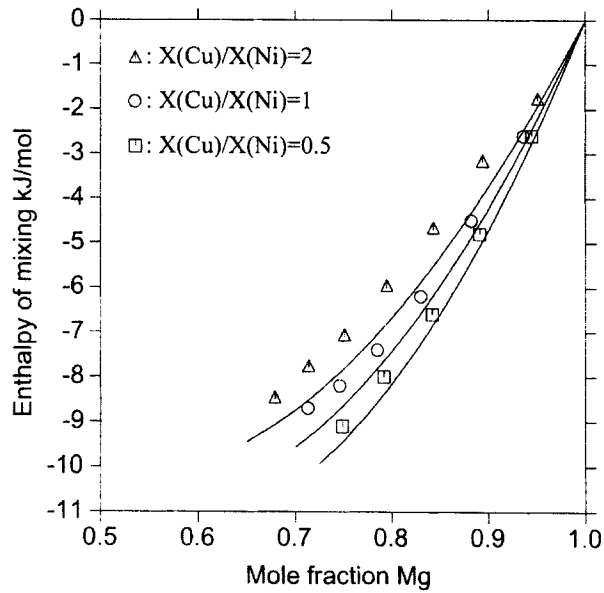


Figure 8: Calculated enthalpy of mixing in the liquid phase at 1008 K from the present work, compared with the experiments by Feufel et al. [18].

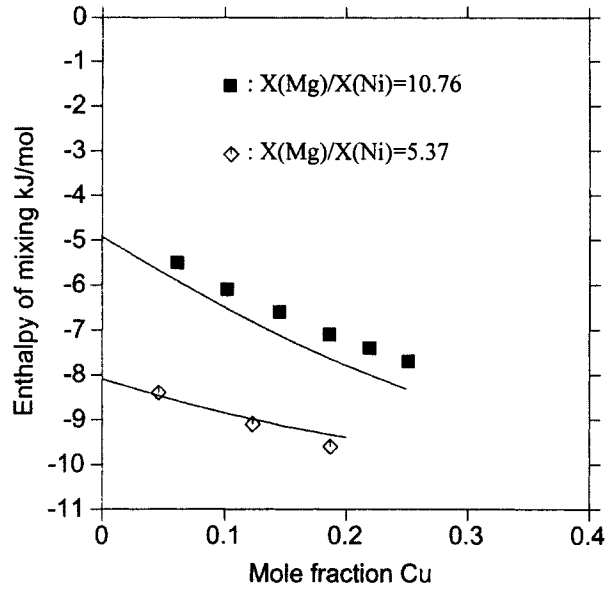


Figure 9: Calculated enthalpy of mixing in the liquid phase at 1008 K from the present work, compared with the experiments by Feufel et al. [18].

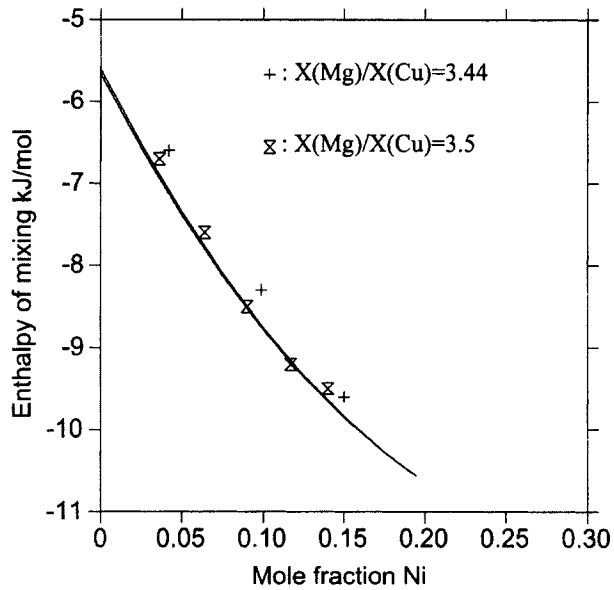


Figure 10: Calculated enthalpy of mixing in the liquid phase at 1008 K from the present work, compared with the experiments by Feufel et al. [18].

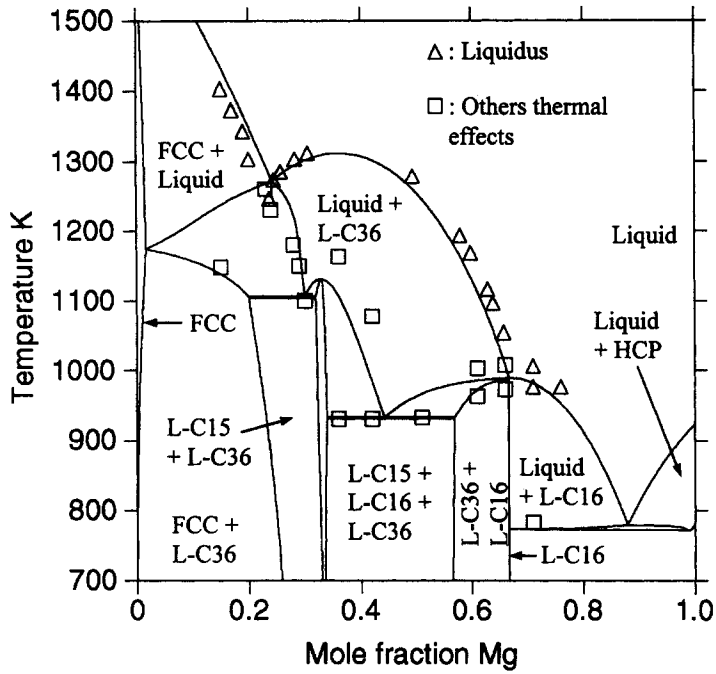


Figure 11: Calculated isopleth for  $X(\text{Cu})/X(\text{Ni})=0.5$ , compared with the experimental data by Ipsier et al. [11].

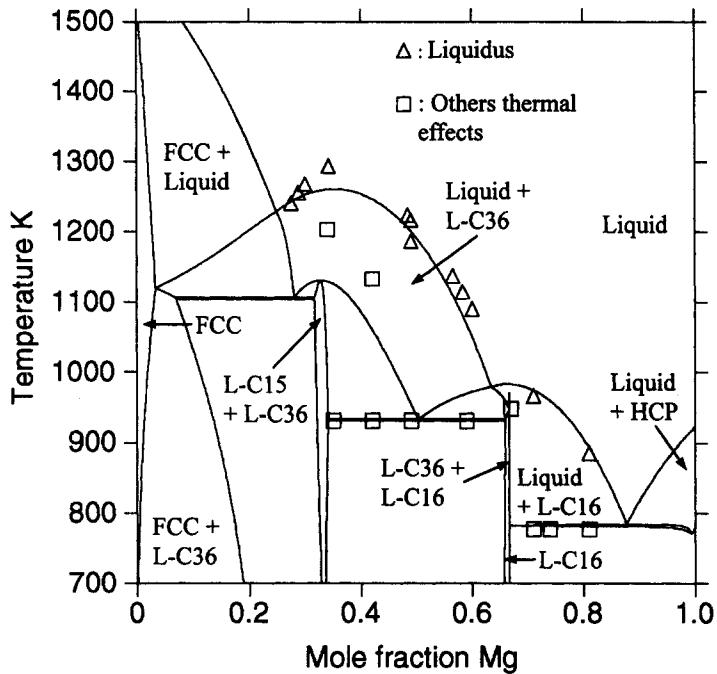


Figure 12: Calculated isopleth for  $X(\text{Cu})/X(\text{Ni})=1$ , compared with the experimental data by Ipsier et al. [11].

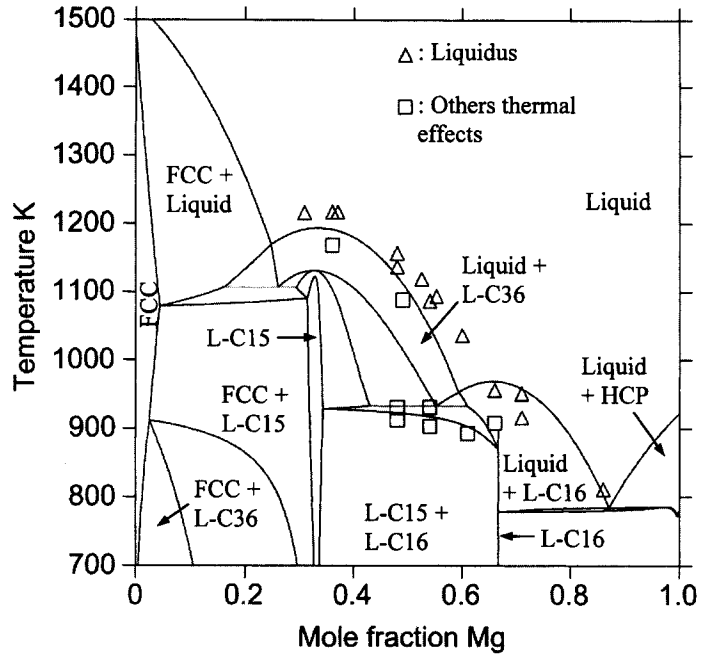


Figure 13: Calculated isopleth for  $X(\text{Cu})/X(\text{Ni})=2$ , compared with the experimental data by Ipsier et al. [11].

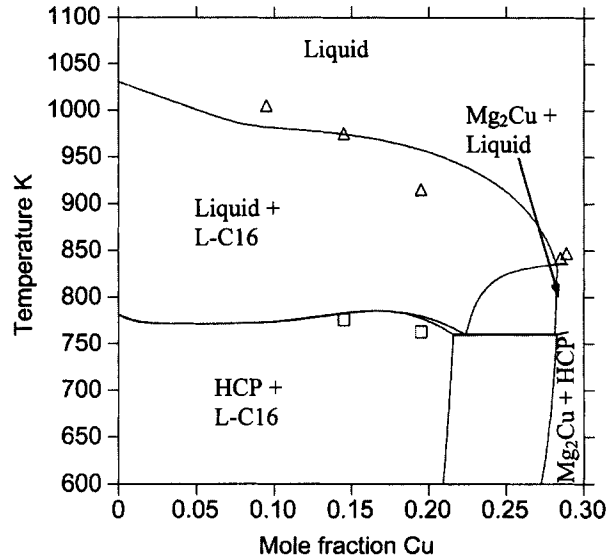


Figure 14: Calculated isopleth for  $X(\text{Mg})=0.71$  at.%, compared with the experimental data by Ipsier et al. [11].

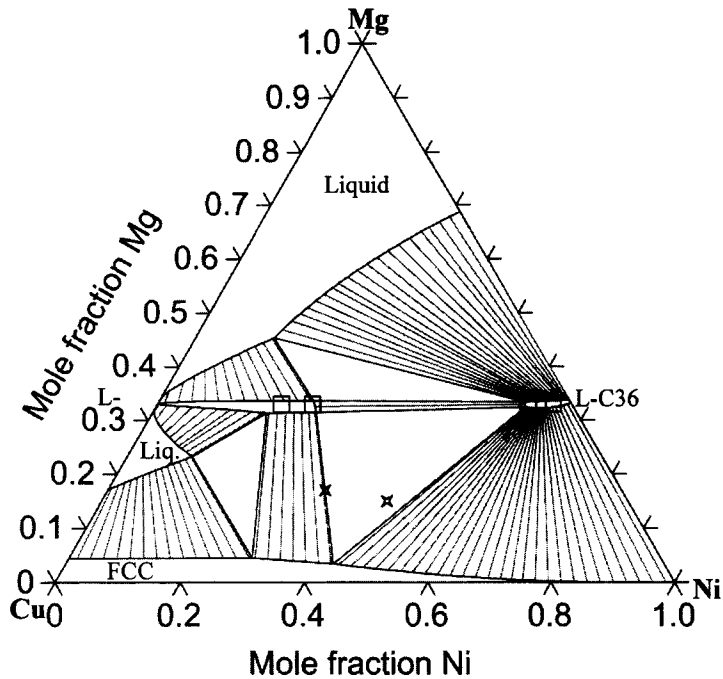


Figure 15: Calculated isothermal section at 1073 K, compared with the experimental data from ref. [10].

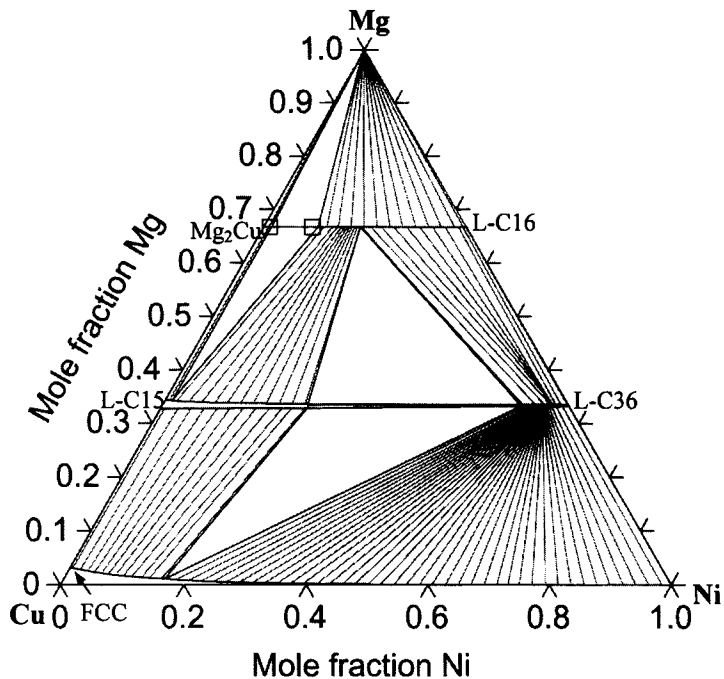


Figure 16: Calculated isothermal section at 673 K, compared with the experimental data from ref. [12].